

## Godunov Method for Stefan Problems with Enthalpy Formulations

D. Tarwidi<sup>1,\*</sup> and S.R. Pudjaprasetya<sup>2</sup>

<sup>1</sup> *Department of Computational Science, Faculty of Mathematics and Natural Sciences, Institut Teknologi Bandung, Jalan Ganesha 10, Bandung 40132, Indonesia.*

<sup>2</sup> *Industrial and Financial Mathematics Research Group, Faculty of Mathematics and Natural Sciences, Institut Teknologi Bandung, Jalan Ganesha 10, Bandung 40132, Indonesia.*

*Received 3 May 2013; Accepted (in revised version) 20 May 2013*

*Available online 31 May 2013*

---

**Abstract.** A Stefan problem is a free boundary problem where a phase boundary moves as a function of time. In this article, we consider one-dimensional and two-dimensional enthalpy-formulated Stefan problems. The enthalpy formulation has the advantage that the governing equations stay the same, regardless of the material state (liquid or solid). Numerical solutions are obtained by implementing the Godunov method. Our simulation of the temperature distribution and interface position for the one-dimensional Stefan problem is validated against the exact solution, and the method is then applied to the two-dimensional Stefan problem with reference to cryosurgery, where extremely cold temperatures are applied to destroy cancer cells. The temperature distribution and interface position obtained provide important information to control the cryosurgery procedure.

**AMS subject classifications:** 65M10, 78A48

**Key words:** Stefan problems, Godunov method, solidification, enthalpy, cryosurgery.

---

### 1. Introduction

Stefan problems describe phase change moving boundaries, such as in solidification and melting processes. Their main characteristic is that the location of the interface between two phases is unknown, and must be determined as part of the solution. After Josef Stefan compared his calculations for the melting of the polar ice cap with the existing observational data around 1890, Stefan problems were soon found to be important in many other areas of the natural sciences and elsewhere. In industrial processes, Stefan problems

---

\*Corresponding author. *Email addresses:* dede.tarwidi@yahoo.com (D. Tarwidi), sr\_pudjap@math.itb.ac.id (S.R. Pudjaprasetya)

occur in metal solidification, food freezing, and ice production. In medical science, the Stefan problem arises in cryosurgery, where in particular cancer cells may be destroyed under extremely cold temperatures.

In Stefan problems where the heat conduction equation is to be solved in both solid and liquid regions, the moving boundary or interface that separates the two regions presents a major difficulty. Analytical solutions are very limited, even for one-dimensional problems. Alexiades & Solomon [1] have discussed in detail the analytical and numerical solution of one-dimensional and two-dimensional Stefan problems.

There have been many methods developed to solve moving boundary problems more generally, including the enthalpy method, the boundary immobilisation method and perturbation, nodal integral and heat balance integral methods [2]. However, the enthalpy method is the most widely used in solving Stefan problems [3–5], as its strength lies in reformulating the heat conduction equations to involve the internal energy (enthalpy). Thus in the enthalpy reformulation the governing equation stays the same for any phase — whether solid, liquid, or even gas. In corresponding discrete formulations, the conservative property of the system is directly preserved in the difference equations. In particular, the finite volume method can thereby simulate the discontinuous solutions with correct speeds, and automatically predict the moving interfaces.

In this article, the first-order Godunov method is adopted to solve the Stefan problem. Comprehensive reviews of the Godunov method can be found in Refs. [6–10]. In Section 2, the exact solution of the one-dimensional solidification problem is used to test our implementation, which is then applied to simulate the two-dimensional system in Section 3.

## 2. One-Dimensional Stefan Problem

In this section, we first discuss the mathematical formulation and the analytical solution of the one-dimensional Stefan problem, and then compare the results we obtain using the Godunov method in the enthalpy formulation.

### 2.1. Mathematical formulation and analytical solution

Consider a one-dimensional container of length  $l$ , full of liquid with a freezing temperature  $T_m$ . Suppose the initial temperature of the liquid  $T_L$  is higher than  $T_m$ , and one end of the liquid  $x = 0$  is maintained at temperature  $T_S (< T_m)$  for  $t > 0$ , whereas the other end  $x = l$  is insulated. The solidification process consequently starts from  $x = 0$ , and extends over increasing intervals as the time  $t$  increases (a well-known Stefan problem). We assume that the material density  $\rho$  is constant; and the thermophysical properties are the latent heat  $L$ , the respective specific heats of the liquid and solid  $c_L$  and  $c_S$ , and the respective thermal conductivities of the liquid and solid  $k_L$  and  $k_S$ .

Suppose  $X(t)$  is the interface that separates the two regions at time  $t$ , such that  $0 \leq x < X(t)$  is the solid region and  $X(t) < x \leq l$  is the liquid region — cf. Fig. 1. Our aim is to determine the temperature distribution  $T(x, t)$  throughout the material, and the interface position  $X(t)$ . Heat conduction in the solid and liquid regions obeys the respective

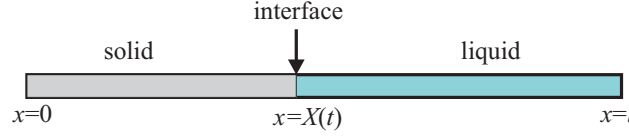


Figure 1: Configuration for the one-dimensional Stefan problem.

diffusion equations

$$\rho c_S T_t = k_S T_{xx}, \quad 0 < x < X(t), \quad t > 0 \quad (\text{solid}) \quad (2.1)$$

and

$$\rho c_L T_t = k_L T_{xx}, \quad X(t) < x < l, \quad t > 0 \quad (\text{liquid}). \quad (2.2)$$

At the interface  $X(t)$ , conservation of heat flux yields

$$\rho L X'(t) = k_S T_x(X(t)^-, t) - k_L T_x(X(t)^+, t), \quad t > 0, \quad (2.3)$$

where the temperature at the interface is

$$T(X(t), t) = T_m, \quad t > 0. \quad (2.4)$$

The initial condition and boundary conditions are

$$T(x, 0) = T_L > T_m, \quad 0 < x \leq l, \quad X(0) = 0, \quad (2.5)$$

$$T(0, t) = T_S < T_m, \quad T_x(l, t) = 0, \quad t > 0. \quad (2.6)$$

The analytical solution of the above Stefan problem for the semi-infinite domain  $x \geq 0$  is [1]

$$T(x, t) = \begin{cases} T_S + (T_m - T_S) \frac{\operatorname{erf}\left(\frac{x}{\sqrt{2\alpha_S t}}\right)}{\operatorname{erf}(\lambda)}, & 0 < x < X(t), \quad t > 0 \\ T_L - (T_L - T_m) \frac{\operatorname{erfc}\left(\frac{x}{\sqrt{2\alpha_L t}}\right)}{\operatorname{erfc}\left(\lambda \sqrt{\alpha_S/\alpha_L}\right)}, & x > X(t), \quad t > 0 \end{cases} \quad (2.7)$$

and

$$X(t) = 2\lambda \sqrt{\alpha_S t}, \quad t > 0. \quad (2.8)$$

Here the parameter  $\lambda$  is a solution of the transcendental equation

$$\frac{St_S}{\exp(\lambda^2)\operatorname{erf}(\lambda)} - \frac{St_L}{\exp(v^2\lambda^2)\operatorname{erf}(v\lambda)} = \lambda\sqrt{\pi}, \quad (2.9)$$

where

$$\alpha_S = \frac{k_S}{\rho c_S}, \quad St_S = \frac{c_S(T_m - T_S)}{L}, \quad St_L = \frac{c_L(T_L - T_m)}{L}, \quad v = \sqrt{\frac{\alpha_S}{\alpha_L}}. \quad (2.10)$$

As previously mentioned, this analytical solution will now be used to test our numerical implementation.

## 2.2. Enthalpy formulation and Godunov method

As indicated, our two-phase Stefan problem involves solving heat conduction equations in the solid and liquid regions simultaneously, where the boundary or interface is moving so that the numerical solution is not straightforward. We first reformulate the heat conduction equations in terms of internal energy (enthalpy), as follows.

Suppose  $E(x, t)$  denotes the enthalpy per unit length at position  $x$  and time  $t$ , the sum of sensible heat and latent heat — i.e.

$$E(x, t) = \begin{cases} \int_{T_m}^{T(x,t)} \rho c_S(\tau) d\tau, & T(x, t) < T_m \quad (\text{solid}), \\ \int_{T_m}^{T(x,t)} \rho c_L(\tau) d\tau + \rho L, & T(x, t) > T_m \quad (\text{liquid}). \end{cases} \quad (2.11)$$

If  $c_S$  and  $c_L$  are constants, then (2.11) becomes

$$E(x, t) = \begin{cases} \rho c_S(T(x, t) - T_m), & T(x, t) < T_m, \\ \rho c_L(T(x, t) - T_m) + \rho L, & T(x, t) > T_m, \end{cases} \quad (2.12)$$

as illustrated in Fig. 2. Moreover, we can express  $T(x, t)$  in terms of  $E(x, t)$  as follows:

$$T(x, t) = \begin{cases} T_m + \frac{E(x, t)}{\rho c_S}, & E(x, t) \leq 0 \quad (\text{solid}), \\ T_m, & 0 < E(x, t) < \rho L \quad (\text{interface}), \\ T_m + \frac{E(x, t) - \rho L}{\rho c_L}, & E(x, t) \geq \rho L \quad (\text{liquid}). \end{cases} \quad (2.13)$$

Here we assume the densities of the solid and liquid are the same ( $\rho = \rho_S = \rho_L$ ), so there is no volume expansion during the process.

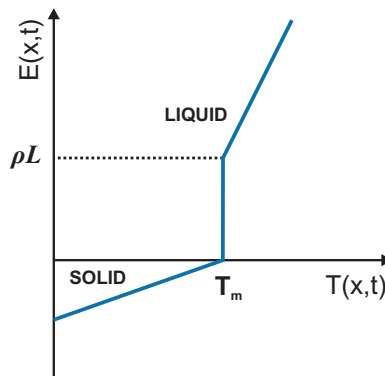


Figure 2: Enthalpy with respect to temperature, and the phase states.

For the computation, the fluid domain  $[0, l]$  is divided into  $M$  subregions called control volumes — viz.  $V_i, i = 1, 2, \dots, M$ . Each control volume  $V_i$  is associated with a point  $x_i$

located at the midpoint of its respective interval — cf. Fig. 3. Conservation of energy in each control volume  $V_i = [x_{i-1/2}, x_{i+1/2}]$  is represented by

$$\int_{x_{i-1/2}}^{x_{i+1/2}} [E(x, t + \Delta t) - E(x, t)] dx = \int_t^{t+\Delta t} [q(x_{i-1/2}, t) - q(x_{i+1/2}, t)] dt \quad (2.14)$$

where  $q(x, t) = -kT_x$ , with  $k = k_S$  in the solid region and  $k = k_L$  in the liquid region.

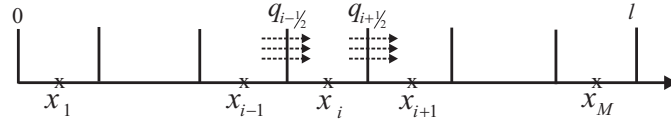


Figure 3: Discretisation of the computational domain into  $M$  control volumes.

From the Mean Value Theorem

$$E(x_i, t) \approx \frac{1}{\Delta x} \int_{x_{i-1/2}}^{x_{i+1/2}} E(x, t) dx ,$$

hence Eq. (2.14) yields

$$[E(x_i, t + \Delta t) - E(x_i, t)] \Delta x = \int_t^{t+\Delta t} [q(x_{i-1/2}, t) - q(x_{i+1/2}, t)] dt . \quad (2.15)$$

From Eq. (2.15), we have the explicit scheme

$$E_i^{n+1} = E_i^n + \frac{\Delta t}{\Delta x} [q_{i-1/2}^n - q_{i+1/2}^n] , \quad (2.16)$$

where

$$q_{i-1/2} = -\frac{T_i - T_{i-1}}{R_{i-1/2}} , \quad R_{i-1/2} = \frac{1}{2} \Delta x \left( \frac{1}{k_{i-1}} + \frac{1}{k_i} \right) . \quad (2.17)$$

This scheme can handle a discontinuous solution automatically, and the enthalpy  $E$  is expected to be discontinuous at the interface due to the different thermal properties in each phase. Note that the formula in Eq. (2.17) reduces to

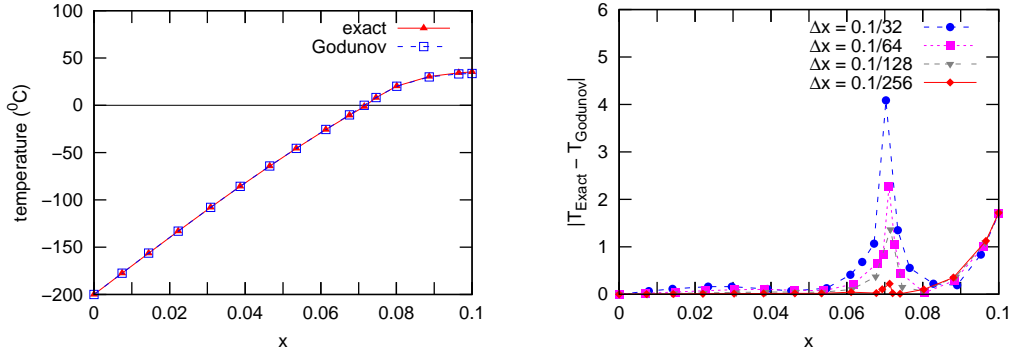
$$q_{i-1/2} = -k_S \frac{T_i - T_{i-1}}{\Delta x} \text{ in the solid region, and}$$

$$q_{i-1/2} = -k_L \frac{T_i - T_{i-1}}{\Delta x} \text{ in the liquid region .}$$

The one-dimensional solidification problem described in Section 2.1 is now simulated, assuming the liquid phase is water. We assume that  $l = 0.1$  m,  $T_L = 37^\circ\text{C}$ , and  $T_S = -200^\circ\text{C}$  ( $x = 0.1$  is the insulated end). The corresponding initial enthalpy is  $E(x, 0) = \rho c_L(T_L - T_m) + \rho L$ , and the other physical properties are given in Table 1.

Table 1: Physical properties of water.

symbol	parameter	value	unit
$c_s$	specific heat of solid	1.7	kJ/kg/K
$c_l$	specific heat of liquid	4.1868	kJ/kg/K
$k_s$	thermal conductivity of solid	$2.66 \cdot 10^{-3}$	kJ/m/s/K
$k_l$	thermal conductivity of liquid	$0.6 \cdot 10^{-3}$	kJ/m/s/K
$T_m$	freezing point	273	K
$L$	latent heat	333.73	kJ/kg
$\rho$	density	1000	kg/m <sup>3</sup>

(a) Temperature distribution at  $t = 50$  minutes calculated using  $\Delta x = 0.1/128$ .(b) Error of temperature distribution at  $t = 50$  minutes, for  $\Delta x = 0.1/32$ ,  $\Delta x = 0.1/64$ ,  $\Delta x = 0.1/128$ ,  $\Delta x = 0.1/256$ .Figure 4: (a) Temperature distribution with  $\Delta x = 0.1/128$ . (b) Error of temperature distribution for  $\Delta x = 0.1/32$ ,  $\Delta x = 0.1/64$ ,  $\Delta x = 0.1/128$ ,  $\Delta x = 0.1/256$ .

The temperature distribution on 128 nodes is shown in Fig. 4(a), and the corresponding error for the temperature distribution values in Fig. 4(b). The error reduces as the number of nodes increases, although it is not so small near the interface and the boundary  $x = 0.1$ . At the interface, this is because we approximate the heat flux by first-order finite differences; and at the boundary, because the numerical computation is implemented on a finite domain whereas the analytical solution is for a semi-infinite domain.

The position  $x_p(t)$  of the interface at any time  $t$  is defined by  $T(x_p(t), t) = 0$ , and is not necessarily at the grid points — cf. Fig. 4(a). A discontinuous enthalpy value indicates a cell that contains the interface, and when the interface is located in the cell  $V_i = [x_{i-1/2}, x_{i+1/2}]$  we approximate the interface position as follows. First, we define the liquid fraction in a control volume  $V_i$  — i.e.

$$\lambda_i^n = \begin{cases} 0, & E_i^n \leq 0 & \text{(solid)}, \\ \frac{E_i^n}{\rho L}, & 0 < E_i^n < \rho L & \text{(interface)}, \\ 1, & E_i^n \geq \rho L & \text{(liquid)}, \end{cases} \quad (2.18)$$

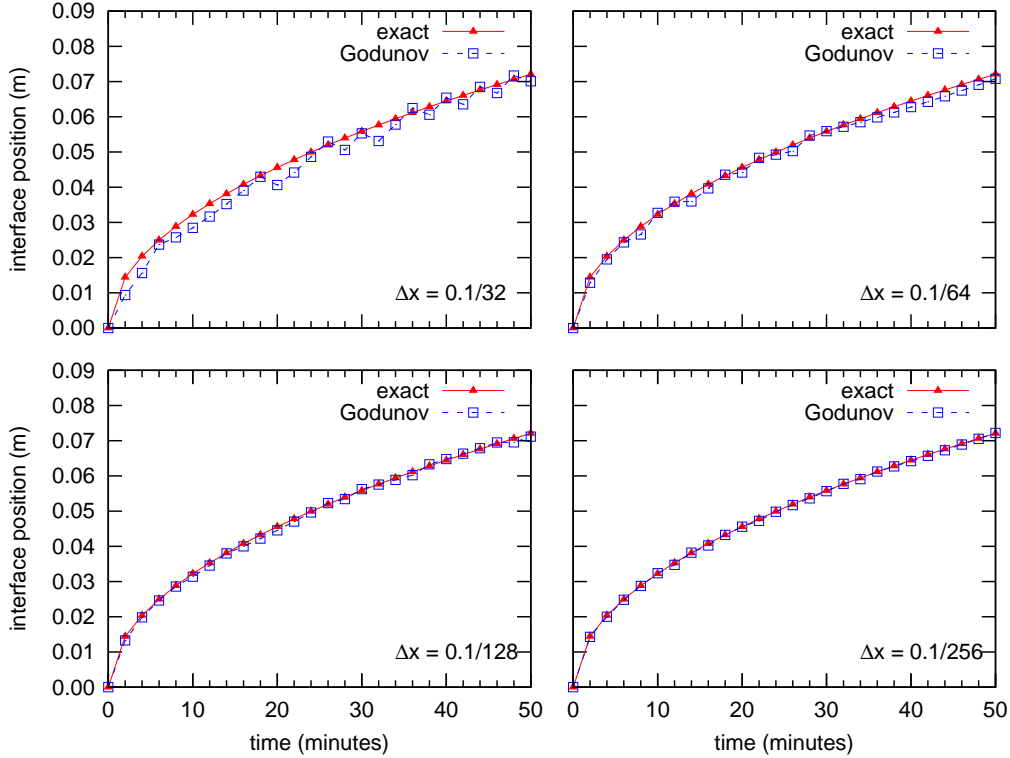


Figure 5: Interface position. Image order from top left to bottom right:  $\Delta x = 0.1/32$ ,  $\Delta x = 0.1/64$ ,  $\Delta x = 0.1/128$ , and  $\Delta x = 0.1/256$ .

where  $0 \leq \lambda_i \leq 1$ . Thus the value  $\lambda_i = 0$  means the control volume  $V_i$  contains 100% solid, whereas  $\lambda_i = 0.25$  means it contains 25% liquid and 75% solid. At any time  $t_n$ ,  $\lambda_m^n = E_m^n / \rho L$  represents the liquid fraction in  $V_m$ , when the interface position is

$$X^n = x_{m-1/2} + \lambda_m^n \Delta x_m. \quad (2.19)$$

In Fig. 5, the interface positions obtained numerically from Eq. (2.19) are shown, together with the analytical interface given by Eq. (2.8). As more nodes are used, it is seen that the numerical solution we obtained from the Godunov method is closer to the exact solution.

### 3. Two-Dimensional Stefan Problem with a Cryosurgery Application

In this section, the numerical implementation for the one-dimensional Stefan problem is extended to two dimensions. Our simulation for the two-dimensional Stefan problem is in the context of a cryosurgery procedure, where extremely cold temperatures are used to destroy cancer cells. When liquid nitrogen at a temperature of  $-200^\circ\text{C}$  is injected into cancer cells through a device called a cryoprobe, an important aspect of the procedure is

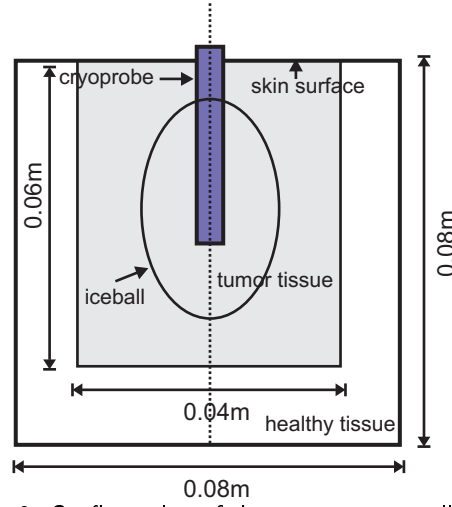


Figure 6: Configuration of the cryosurgery application.

to maximise the destruction of tumour tissue and simultaneously minimise the damage to surrounding healthy tissue [11, 12].

Let us suppose that the size of the tumour tissue to be destroyed is  $0.04 \text{ m} \times 0.06 \text{ m}$ , and it is located in healthy tissue with size  $0.08 \text{ m} \times 0.08 \text{ m}$ . A cryoprobe with diameter  $3 \text{ mm}$  is put into the middle of the tumour tissue as shown in Fig. 6, and liquid nitrogen is injected through the cryoprobe such that an ice ball crystal or solidification is formed around it and solidification extends into the surrounding tumour tissue. The tumour tissue will be destroyed if its temperature reaches  $-20^\circ\text{C}$  to  $-30^\circ\text{C}$ . The time needed to freeze cancer cells depends upon the position of the cryoprobe, their distance to the cryoprobe, and thermophysical properties. In this study, the cryosurgery procedure is considered to last for 800 seconds, and is then followed by reheating the frozen tissue on producing a temperature of  $80^\circ\text{C}$  in the cryoprobe.

Such cryosurgery is an example of a two-phase Stefan problem. If the two-dimensional domain is defined by  $0 \leq x \leq l_1$  and  $0 \leq y \leq l_2$ , let us consider the case when  $l_1 = l_2 = 0.08 \text{ m}$ . We divide  $[0, l_1]$  and  $[0, l_2]$  into  $M_1$  and  $M_2$  subintervals respectively, so there are  $M_1 M_2$  control volumes  $V_{i,j}$ . The conservation of energy in each control volume  $V_{i,j} = [x_{i-1/2}, x_{i+1/2}] \times [y_{j-1/2}, y_{j+1/2}]$  is

$$\int_{V_{i,j}} [E(\mathbf{x}, t + \Delta t) - E(\mathbf{x}, t)] \, dA = \int_t^{t+\Delta t} \int_{\partial V_{i,j}} -\mathbf{q} \cdot \hat{\mathbf{n}} \, dS \, dt, \quad (3.1)$$

where  $E(\mathbf{x}, t)$  is the enthalpy per unit area,  $-\mathbf{q} \cdot \hat{\mathbf{n}}$  is the heat flux into the area  $V_{i,j}$  across its boundary  $\partial V_{i,j}$ , where  $\hat{\mathbf{n}}$  denotes the outward unit normal to  $\partial V_{i,j}$ .

As in the one-dimensional case, we apply the Godunov method to the problem represented in terms of the enthalpy. The explicit scheme for this two-dimensional problem is thus

$$E_{i,j}^{n+1} = E_{i,j}^n + \frac{\Delta t}{\Delta x} [q_{i-1/2,j}^n - q_{i+1/2,j}^n] + \frac{\Delta t}{\Delta y} [q_{i,j-1/2}^n - q_{i,j+1/2}^n], \quad (3.2)$$

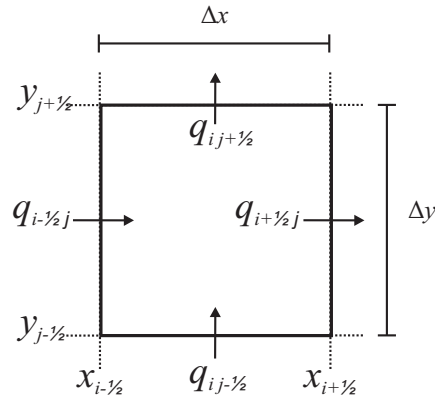


Figure 7: Cell  $V_{i,j}$  in the two-dimensional domain.

where  $q_{i+1/2,j}$  and  $q_{i,j+1/2}$  represent the heat flux crossing vertical and horizontal bound of  $V_{i,j}$ , respectively (cf. Fig. 7).

We assume that the initial tissue temperature is uniform — viz.  $T_c(x, y, 0) = 37^\circ\text{C}$ , which is the healthy human body temperature. Since our problem is symmetric, we need only compute in the right half of the domain. The boundary conditions used are defined in Fig. 8, where  $T_{\text{probe}}(t)$  is the temperature of the cryoprobe surface,  $T_{\text{air}} (= 20^\circ\text{C})$  is the

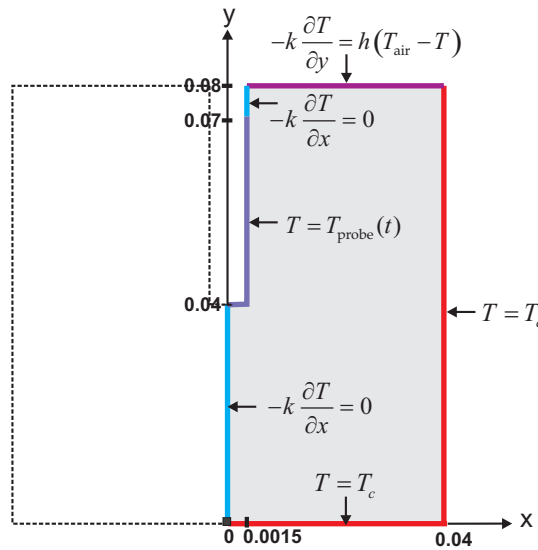


Figure 8: Boundary conditions in the cryosurgery application.

surrounding temperature, and  $h (= 20 \text{ W/m}^2\text{°C})$  is the convective heat transfer coefficient between the skin surface and the surrounding air. The other parameters are given in Table 1. We also assume that: (a) the healthy tissue and the tumour tissue have the same thermal properties; and (b) the frozen and unfrozen tissue have same density, so that there

is no volume expansion.

The simulation results are expected to help a surgeon predict the temperature distribution required before the tumour surgery is performed, so that damage to healthy tissue can be minimised. The temperature distribution during the cryosurgery procedure as a function of time is shown in Fig. 9, where the freezing process is seen to start from the tissue adjoining the cryoprobe and then move outwards into its surroundings. The contour plot in Fig. 9 represents the interface as a function of time, obtained from interpolating  $T(x, y, t) = 0^\circ\text{C}$  (freezing point) using cubic splines. The inner region of the contour curve shows the area of the ice ball, and on knowing the growth of the ice ball one can determine how much of the tumour tissue has been frozen and minimise the damage to the healthy tissue. After the 800 seconds of the freezing process, the frozen tissue is reheated by the flow of a certain gas with temperature  $80^\circ\text{C}$  into the cryoprobe. The temperature distribution during the reheating process and the melting of the ice ball with time is shown in Fig. 10.

#### 4. Conclusion

We have shown that the enthalpy formulation for our Stefan problems is suitable for a finite volume discretisation that accounts for the moving boundaries. For the one-dimensional Stefan problem, the first-order Godunov method produces relatively small error, which reduces as more nodes were used (the larger errors occur near the interface and the right boundary). The Godunov method was then applied to the two-dimensional Stefan problem, with application to cryosurgery. The simulation provides the temperature distribution for a two-dimensional tissue model, and the interface position that is important information to control the cryosurgery procedure. In brief, the Godunov method employed was found suitable to solve the one-dimensional and two-dimensional Stefan problems numerically, and the future development of a second-order Godunov method may be expected to produce even more accurate numerical results.

#### Acknowledgments

We would like to thank Prof. Robert Eymard, who first introduced us to the finite volume approach for Stefan problems. We acknowledge financial support from Riset KK ITB Grant No. 242/I.1.C01/PL/2013, and partially from Riset KK ITB Grant No. 232/I.1.C01/PL/2013.

#### References

- [1] V. ALEXIADES AND A.D. SOLOMON, *Mathematical Modelling of Melting and Freezing Processes*, Hemisphere Publishing Corporation, Washington DC, 1981.
- [2] J. CALDWELL AND Y.Y. KWAN, *Numerical methods for one-dimensional Stefan problems*, *Communications in Numerical Methods in Engineering*, 20 (2004), pp. 535–545.

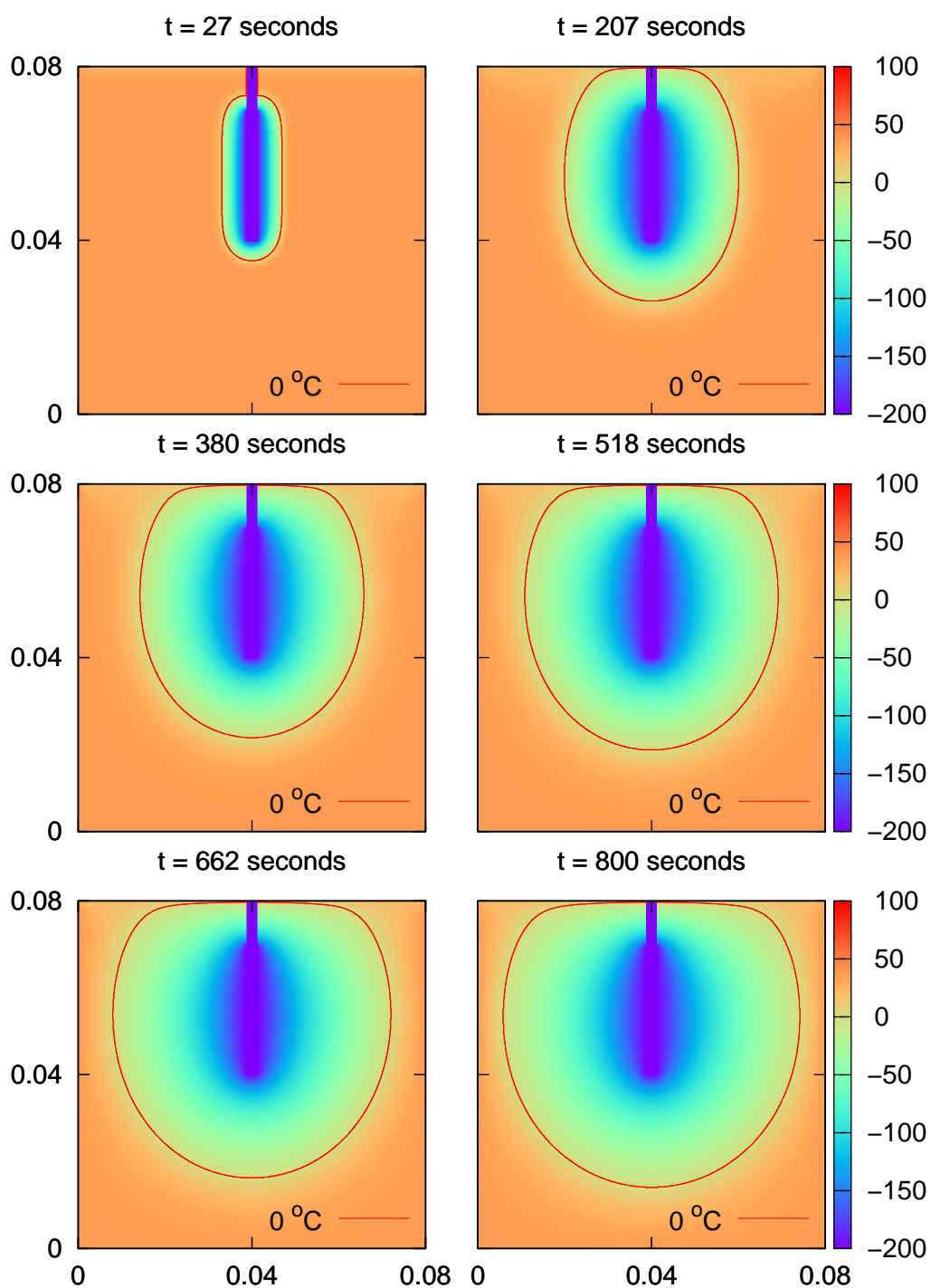


Figure 9: Temperature distribution and interface position during the cryosurgery procedure. Image order from top left to bottom right:  $t = 17$ ,  $t = 207$ ,  $t = 380$ ,  $t = 518$ ,  $t = 662$ ,  $t = 800$  seconds.

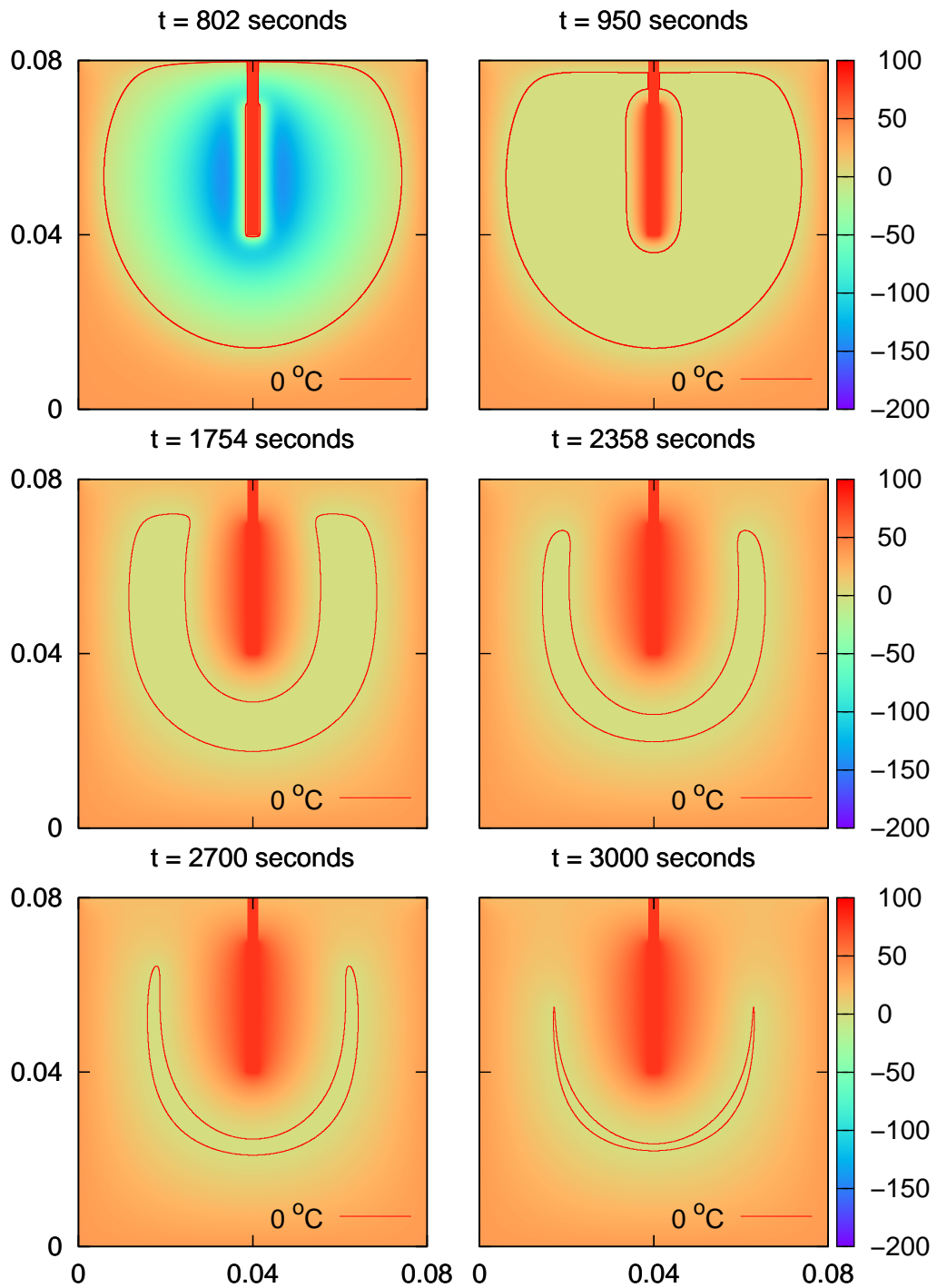


Figure 10: Temperature distribution and interface position during the heating process. Image order from top left to bottom right:  $t = 802$ ,  $t = 950$ ,  $t = 1754$ ,  $t = 2358$ ,  $t = 2700$ ,  $t = 3000$  seconds.

- [3] V.R. VOLLER AND L. SHADABI, *Enthalpy methods for tracking a phase change boundary in two dimensions*, International Communications in Heat and Mass Transfer, 11 (1984), pp. 239–249.
- [4] V. VOLLER AND M. CROSS, *Accurate solutions of moving boundary problems using the enthalpy method*, International Journal of Heat and Mass Transfer, 24 (1981), pp. 545–556.
- [5] A. ESEN AND S. KUTLUAY, *A numerical solution of the Stefan problem with a Neumann-type boundary condition by enthalpy method*, Applied Mathematics and Computation, 148 (2004), pp. 321–329.
- [6] R.J. LEVEQUE, *Finite-Volume Methods for Hyperbolic Problems*, Cambridge University Press, Cambridge, 2002.
- [7] E.F. TORO, *Riemann Solvers and Numerical Methods for Fluid Dynamics: A Practical Introduction*, Springer-Verlag, Berlin, Heidelberg, 2009.
- [8] B. WENDROFF, *Approximate Riemann solvers, Godunov schemes and contact discontinuities*, in *Godunov Methods: Theory and Applications*, E.F. Toro (ed.), Kluwer Academic/Plenum Publishers, New York, 2001.
- [9] P. COLELLA, *Volume-of-fluid methods for partial differential equations*, in *Godunov Methods: Theory and Applications*, E.F. Toro (ed.), Kluwer Academic/Plenum Publishers, New York, 2001.
- [10] B. VAN LEER, *Upwind and high-resolution methods for compressible flow: From donor cell to residual-distribution schemes*, Communication in Computational Physics, 1 (2006), pp. 192–206.
- [11] G. ZHAO, ET.AL, *Comparative study of the cryosurgical processes with two different cryosurgical systems: the endocare cryoprobe system versus the novel combined cryosurgery and hyperthermia system*, Latin American Applied Research, 37 (2007), pp. 215–222.
- [12] S. KUMAR AND V.K. KATIYAR, *Numerical study on phase change heat transfer during combined hyperthermia and cryosurgical treatment of lung cancer*, International Journal of Applied Mathematics and Mechanics, 3 (2007), pp. 1–17.